

3D hierarchical porous carbon matching ionic liquid with  
ultrahigh specific surface area and appropriate porous  
distribution for supercapacitors

Quanzhou Du, Yuhua Zhao, Kelei Zhuo,\* Yujuan Chen, Lifang Yang, Chunfeng  
Wang, and Jianji Wang\*

## 1. Electrochemical Measurements

The complex form of capacitance  $C(\omega)$  is dependent on the real part of the capacitance  $C'(\omega)$  and the imaginary part of the capacitance  $C''(\omega)$ , which is defined as follows

$$C(\omega) = C'(\omega) - jC''(\omega) \quad (1)$$

$$C'(\omega) = \frac{-Z''(\omega)}{\omega|Z(\omega)|^2} \quad (2)$$

$$C''(\omega) = \frac{Z'(\omega)}{\omega|Z(\omega)|^2} \quad (3)$$

where  $Z'(\omega)$  is the real component and  $Z''(\omega)$  is the imaginary component of the complex impedance, respectively. The angular frequency  $\omega$  is determined by  $\omega = 2\pi f$ .  $\tau_0$  is the relaxation time constant which is calculated by  $\tau_0 = 1/f_0$

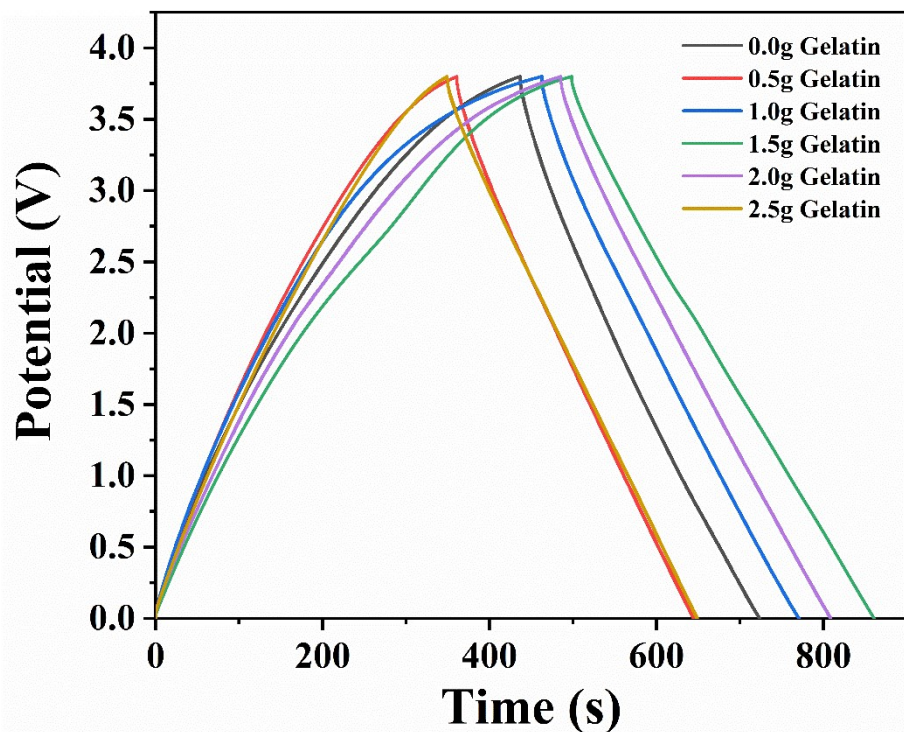


Fig. S1. Galvanostatic charge-discharge (GCD) curves for different dosage of gelatin at  $1 \text{ A g}^{-1}$ .

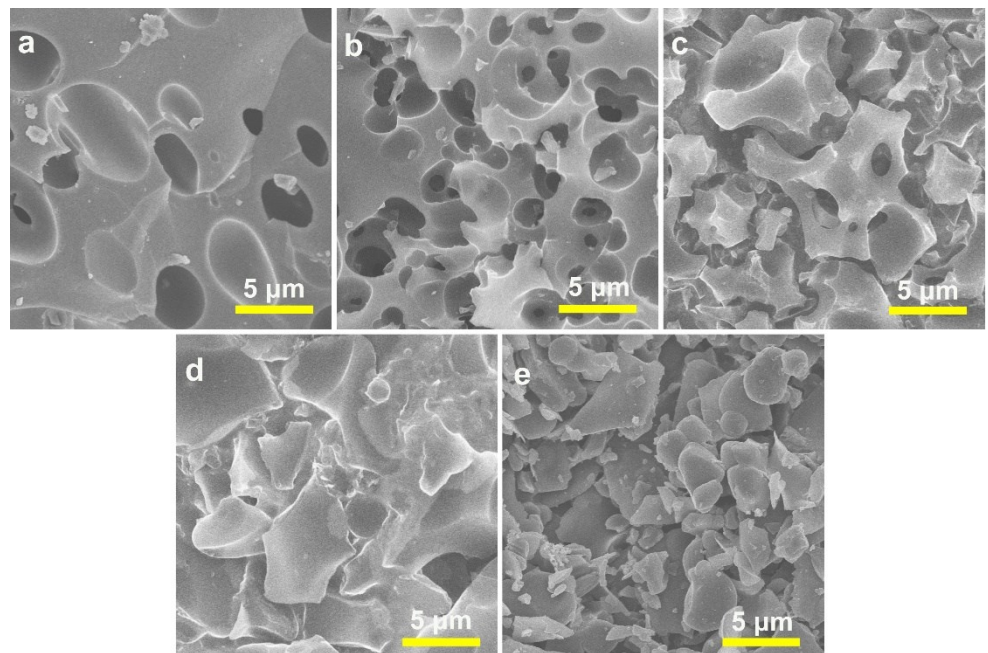


Fig. S2. Morphology characterization of HPC: a) SEM image of HPC-0; b) SEM image of HPC-1.0; c) SEM image of HPC-2.0; d) SEM image of HPC-3.0; e) SEM image of HPC-4.0.

**Table S1** The contents of C element, N element and O element from XPS survey spectra.

Sample	C%	N%	O%
<b>HPC-0</b>	76.44	3.93	19.63
<b>HPC-0.5</b>	83.79	5.46	10.75
<b>HPC-1.0</b>	88.31	2.79	8.90
<b>HPC-1.5</b>	88.54	2.60	8.86
<b>HPC-2.0</b>	86.15	2.55	11.30
<b>HPC-2.5</b>	86.99	2.63	10.38
<b>HPC-3.0</b>	85.48	3.30	11.22
<b>HPC-3.5</b>	83.46	3.15	13.39
<b>HPC-4.0</b>	84.40	3.11	12.49

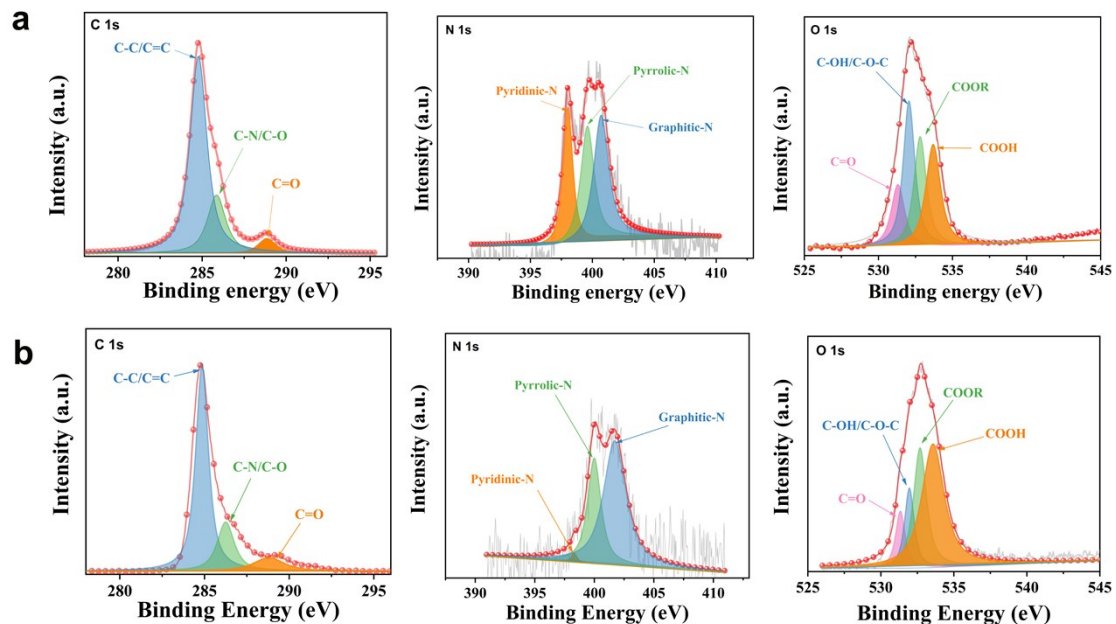


Fig. S3 XPS survey spectra: a) C 1s, N 1s, O 1s spectra of HPC-0; b) C 1s, N 1s, O 1s spectra of HPC-3.5.

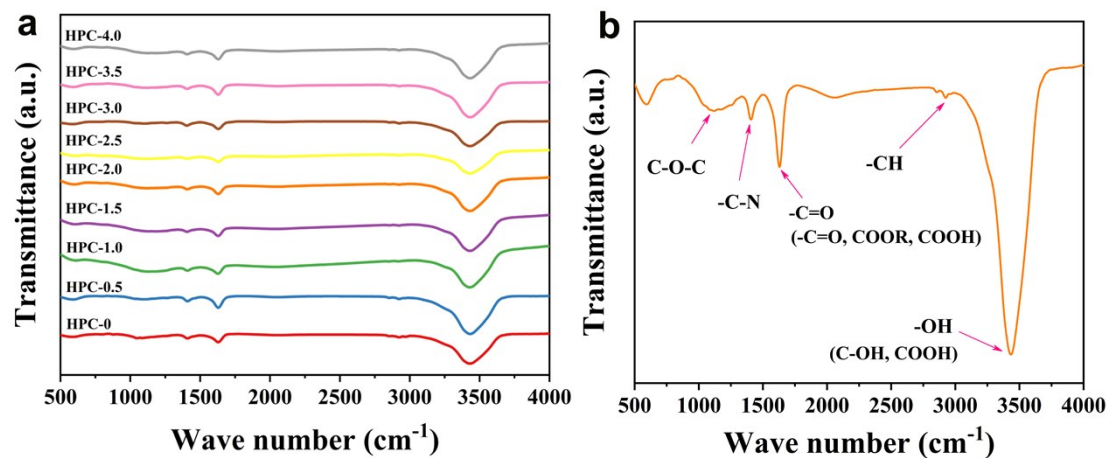


Fig. S4 IR spectroscopy: a) IR spectra of all HPCs; b) IR spectra of HPC-3.5.

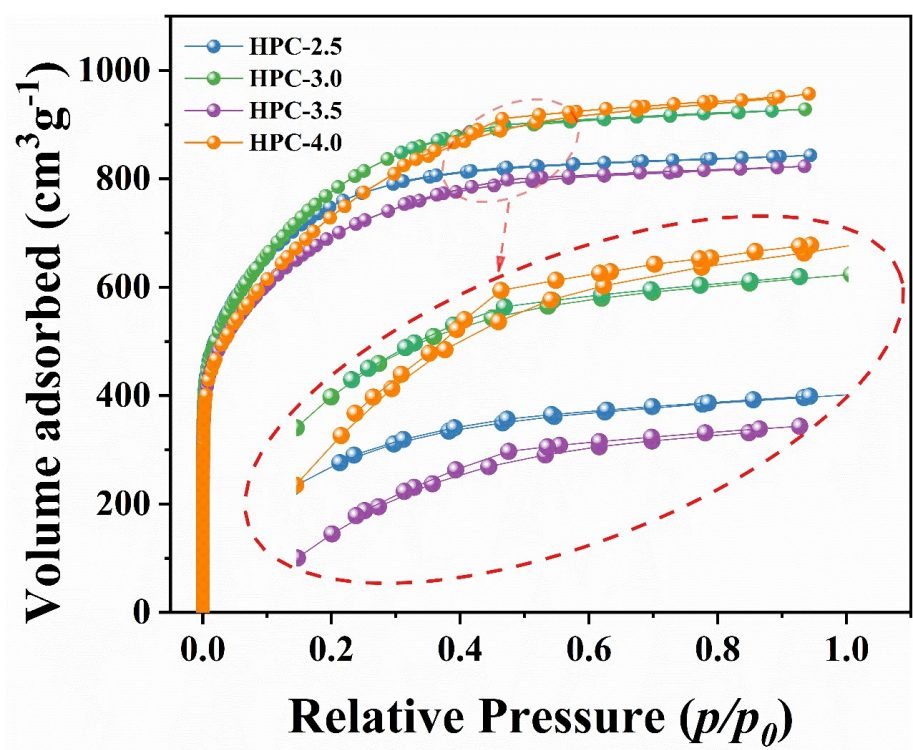


Fig. S5 Magnification of  $\text{N}_2$  adsorption–desorption isotherms.

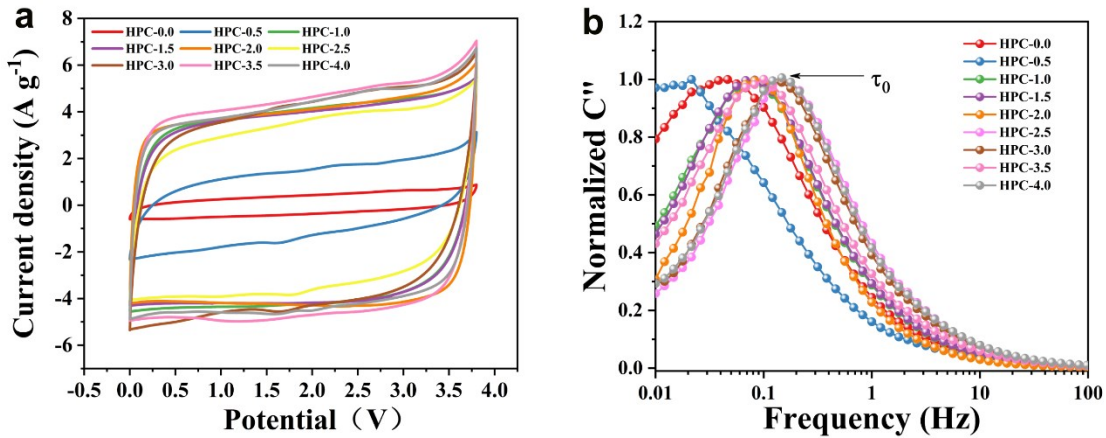


Fig. S6 a) Cyclic voltammetry (CV) curve of all HPC materials at scan rates of  $50 \text{ mv s}^{-1}$ . b) The normalized imaginary part capacitances of all HPC materials.

The same conclusions can be obtained from Fig. S7b as from Fig. 5c: HPC-3.5 has a larger  $\tau_0$  than HPC-3.0 and HPC-4.0 dominated by mesopores, due to a good matching of the micropores size with EMIMBF<sub>4</sub> electrolyte.

**Table S2** Summary of the supercapacitive performance of representative porous carbon electrodes in ionic liquid electrolytes.

Material	IL	Voltage window	Specific capacitance	Reference
mesoporous carbon nanosheets	EMIMBF <sub>4</sub>	3.5 V	130 F g <sup>-1</sup> at 1 A g <sup>-1</sup>	2
mesoporous activated carbon fibers	EMIMBF <sub>4</sub>	4 V	204 F g <sup>-1</sup> at 0.5 A g <sup>-1</sup>	3
porous carbon nanosheets	EMIMBF <sub>4</sub>	3 V	173 F g <sup>-1</sup> at 0.25 A g <sup>-1</sup>	4
ordered mesoporous and microporous carbons	EMIMBF <sub>4</sub>	3.5 V	138 F g <sup>-1</sup> at 0.1 A g <sup>-1</sup>	5
3D cross coupled macro-mesoporous carbon	EMIMBF <sub>4</sub>	4 V	166 F g <sup>-1</sup> at 0.5 A g <sup>-1</sup>	6
salt-templated carbon materials	EMIMBF <sub>4</sub>	3.5 V	178 F g <sup>-1</sup> at 0.2 A g <sup>-1</sup>	7
porosity adjustable graphene monoliths	EMIMBF <sub>4</sub>	4 V	172 F g <sup>-1</sup> at 0.2 A g <sup>-1</sup>	8
N, S dual-doped ordered mesoporous carbon/MnO <sub>2</sub>	EMIMBF <sub>4</sub>	3.5 V	200 F g <sup>-1</sup> at 2 mV s <sup>-1</sup>	9
enteromorpha derived carbons	EMIMBF <sub>4</sub>	3 V	201 F g <sup>-1</sup> at 1 A g <sup>-1</sup>	10
hierarchical porous honeycomb-like carbon	EMIMBF <sub>4</sub>	3.5	174 F g <sup>-1</sup> at 1 A g <sup>-1</sup>	11
highly porous carbon	EMIMBF <sub>4</sub>	4 V	224 A g <sup>-1</sup> at 0.1 A g <sup>-1</sup>	12
HPC	EMIMBF <sub>4</sub>	3.8 V	216.5 A g <sup>-1</sup> at 1 A g <sup>-1</sup>	This work

**Table S3** Summary of energy density and power density of symmetric supercapacitors in ionic liquid electrolytes.

Material	Energy density	Power density	References
mesoporous carbon nanosheets	55.3 Wh kg <sup>-1</sup> 46 Wh kg <sup>-1</sup>	0.87 kW kg <sup>-1</sup> 236 kW kg <sup>-1</sup>	2
mesoporous activated carbon fibers	113 Wh kg <sup>-1</sup> 9.2 Wh kg <sup>-1</sup>	1 kW kg <sup>-1</sup> 83 kW kg <sup>-1</sup>	3
porous carbon nanosheets	54.1 Wh kg <sup>-1</sup> 25.4 Wh kg <sup>-1</sup>	0.375 kW kg <sup>-1</sup> 15 kW kg <sup>-1</sup>	4
ordered mesoporous and microporous carbons	59 Wh kg <sup>-1</sup> 25 Wh kg <sup>-1</sup>	0.1 kW kg <sup>-1</sup> 18 kW kg <sup>-1</sup>	5
3D cross coupled macro-mesoporous carbon	92 Wh kg <sup>-1</sup> 39 Wh kg <sup>-1</sup>	1 kW kg <sup>-1</sup> 200 kW kg <sup>-1</sup>	6
salt-templated carbon materials	76 Wh kg <sup>-1</sup> 39 Wh kg <sup>-1</sup>	0.2 kW kg <sup>-1</sup> 9 kW kg <sup>-1</sup>	7
enteromorpha derived carbons	62 Wh kg <sup>-1</sup> 24 Wh kg <sup>-1</sup>	0.75 kW kg <sup>-1</sup> 60 kW kg <sup>-1</sup>	10
hierarchical porous honeycomb-like carbon	79 Wh kg <sup>-1</sup> 64 Wh kg <sup>-1</sup>	0.87 kW kg <sup>-1</sup> 19.5 kW kg <sup>-1</sup>	11
nanofibrous chitin microspheres	58.7 Wh kg <sup>-1</sup> 38 Wh kg <sup>-1</sup>	0.3 kW kg <sup>-1</sup> 7.1 kW kg <sup>-1</sup>	13
N, O co-doped honeycomb porous carbon	94.1 Wh kg <sup>-1</sup> 42.5 Wh kg <sup>-1</sup>	0.35 kW kg <sup>-1</sup> 17.5 kW kg <sup>-1</sup>	14
3D hierarchical porous carbon materials	46.8 Wh kg <sup>-1</sup> 22.9 Wh kg <sup>-1</sup>	6.2 kW kg <sup>-1</sup> 25.4 kW kg <sup>-1</sup>	15
HPC	108.6 Wh kg <sup>-1</sup> 42.8 Wh kg <sup>-1</sup>	0.96 kW kg <sup>-1</sup> 76.4 kW kg <sup>-1</sup>	This work

## References

1. Taberna, P. L.; Simon, P.; Fauvarque, J. F., Electrochemical Characteristics and Impedance Spectroscopy Studies of Carbon-Carbon Supercapacitors. *Journal of The Electrochemical Society* **2003**, *150* (3), A292.
2. Wang, J.; Xu, Y.; Ding, B.; Chang, Z.; Zhang, X.; Yamauchi, Y.; Wu, K. C., Confined Self-Assembly in Two-Dimensional Interlayer Space: Monolayered Mesoporous Carbon Nanosheets with In-Plane Orderly Arranged Mesopores and a Highly Graphitized Framework. *Angew Chem Int Ed Engl* **2018**, *57* (11), 2894-2898.
3. Hurilechaoketu; Wang, J.; Cui, C.; Qian, W., Highly electroconductive mesoporous activated carbon fibers and their performance in the ionic liquid-based electrical double-layer capacitors. *Carbon* **2019**, *154*, 1-6.
4. Chen, C.; Yu, D.; Zhao, G.; Du, B.; Tang, W.; Sun, L.; Sun, Y.; Besenbacher, F.; Yu, M., Three-dimensional scaffolding framework of porous carbon nanosheets derived from plant wastes for high-performance supercapacitors. *Nano Energy* **2016**, *27*, 377-389.
5. Yan, R.; Heil, T.; Presser, V.; Walczak, R.; Antonietti, M.; Oschatz, M., Ordered Mesoporous Carbons with High Micropore Content and Tunable Structure Prepared by Combined Hard and Salt Templating as Electrode Materials in Electric Double-Layer Capacitors. *Advanced Sustainable Systems* **2018**, *2* (2).
6. Li, J.; Wang, N.; Tian, J.; Qian, W.; Chu, W., Cross-Coupled Macro-Mesoporous Carbon Network toward Record High Energy-Power Density Supercapacitor at 4 V. *Advanced Functional Materials* **2018**, *28* (51), 1806153.
7. Yan, R.; Antonietti, M.; Oschatz, M., Toward the Experimental Understanding of the Energy Storage Mechanism and Ion Dynamics in Ionic Liquid Based Supercapacitors. *Advanced Energy Materials* **2018**, *8* (18).
8. Li, H.; Tao, Y.; Zheng, X.; Luo, J.; Kang, F.; Cheng, H.-M.; Yang, Q.-H., Ultra-thick graphene bulk supercapacitor electrodes for compact energy storage. *Energy & Environmental Science* **2016**, *9* (10), 3135-3142.
9. Lai, F.; Feng, J.; Yan, R.; Wang, G.-C.; Antonietti, M.; Oschatz, M., Breaking the Limits of Ionic Liquid-Based Supercapacitors: Mesoporous Carbon Electrodes Functionalized with Manganese Oxide Nanospotches for Dense, Stable, and Wide-Temperature Energy Storage. *Advanced Functional Materials* **2018**, *28* (36).
10. Yu, W.; Wang, H.; Liu, S.; Mao, N.; Liu, X.; Shi, J.; Liu, W.; Chen, S.; Wang, X., N, O-codoped hierarchical porous carbons derived from algae for high-capacity supercapacitors and battery anodes. *Journal of Materials Chemistry A* **2016**, *4* (16), 5973-5983.
11. Deng, X.; Li, J.; Zhu, S.; Ma, L.; Zhao, N., Boosting the capacitive storage performance of MOF-derived carbon frameworks via structural modulation for supercapacitors. *Energy Storage Materials* **2019**, *23*, 491-498.
12. Wang, X.; Li, Y.; Lou, F.; Melandsø Buan, M. E.; Sheridan, E.; Chen, D., Enhancing capacitance of supercapacitor with both organic electrolyte and ionic liquid electrolyte on a biomass-derived carbon. *RSC Advances* **2017**, *7* (38), 23859-23865.
13. Duan, B.; Gao, X.; Yao, X.; Fang, Y.; Huang, L.; Zhou, J.; Zhang, L., Unique elastic N-doped carbon nanofibrous microspheres with hierarchical porosity derived from renewable chitin for high rate supercapacitors. *Nano Energy* **2016**, *27*, 482-491.

14. Song, Z.; Li, L.; Zhu, D.; Miao, L.; Duan, H.; Wang, Z.; Xiong, W.; Lv, Y.; Liu, M.; Gan, L., Synergistic design of a N, O co-doped honeycomb carbon electrode and an ionogel electrolyte enabling all-solid-state supercapacitors with an ultrahigh energy density. *Journal of Materials Chemistry A* **2019**, 7 (2), 816-826.
15. Guo, N.; Li, M.; Sun, X.; Wang, F.; Yang, R., Enzymatic hydrolysis lignin derived hierarchical porous carbon for supercapacitors in ionic liquids with high power and energy densities. *Green Chemistry* **2017**, 19 (11), 2595-2602.